

MELiSSA

Memorandum of Understanding
ECT/FG/MMM/97.012
ESA/ESTEC Contract 13323/98/NL/MV

TECHNICAL NOTE 45.5

**Kinetic and Stoichiometric Analysis of *Rhodospirillum rubrum* Growth
under Carbon Substrate Limitations in Rectangular Photobioreactors**

Version 1
Issue 0

J.-F. CORNET and C.G. DUSSAP

April 2000

. 33 *4 73 40 78 38 - 33 *4 73 40 74 30 - fax 33 *4 73 40 78 29
E-mail : lgcb@gecbio.univ-bpclermont.fr
cornet@gecbio.univ-bpclermont.fr
<http://www.univ-bpclermont.fr/ubp/lqcb>

Document change log

Version	Issue	Date	Observations
0	0	April 2000	Draft version
1	0		Final version

Technical Note 45.5

Kinetic and Stoichiometric Analysis of *Rhodospirillum rubrum* Growth under Carbon Substrate Limitations in Rectangular Photobioreactors

*J.-François CORNET and C. Gilles DUSSAP
Laboratoire de Génie Chimique Biologique
Université Blaise Pascal
24, Avenue des Landais
63177 Aubière Cedex*

April 2000

Content

	<i>Page</i>
Introduction and Objectives	4
1- Kinetic Model	5
2- Stoichiometries - Yields Calculations	9
2.1- Stoichiometries and Yields in the Illuminated Zone	9
2.2- Stoichiometries and Yields in the Dark Efficient Zone	9
2.3- Mean Stoichiometries and Yields	10
3- Materials and Methods	11
4- Results and Discussion	13
4.1- Acetate as Carbon Substrate	14
4.2- Propionate as Carbon Substrate	16
4.3- Butyrate as Carbon Substrate	18
4.4- Isovalerate as Carbon Substrate	20
4.5- Isobutyrate as Carbon Substrate	22

Conclusions and Perspectives	24
Notations	25
References	27

Introduction and Objectives

For the mathematical modeling of photobioreactors (PBRs) it is necessary to understand and formulate the coupling between the metabolism of micro-organisms and the physical phenomenon of light transfer inside the culture medium. PBRs are governed by radiant light energy availability, which is highly heterogeneous within the culture volume (Aiba 1982; Cornet *et al.*, 1992; Cassano *et al.*, 1995; Acien Fernandez *et al.*, 1997). This spatial heterogeneity causes varying local reaction rates, which makes it necessary to derive local equations and calculate the mean volumetric growth rate by integration over the working illuminated volume in the reactor (Cornet *et al.*, 1992; Cornet *et al.*, 1995; Cornet *et al.*, 1998).

The problem of radiative transfer is now well understood and the authors have already proposed a simple monodimensional mathematical model for describing light transfer in PBRs with different shapes (Cornet *et al.*, 1995; Cornet, 1998). This approach has been proved sufficiently accurate in providing models for simulation and predictive control (Cornet *et al.*, 1995, 1998, and 2000).

Coupling light transfer with stoichiometry and rates is a difficult and specific task in modeling PBRs. It was also demonstrated to significantly depend on the considered metabolism, and clearly the main differences appear between photo-autotrophic and photo-heterotrophic micro-organisms (Cornet *et al.*, 1999; Cornet and Albiol, 2000). Preliminary kinetic experimental results obtained on batch cultures of *Rhodospirillum rubrum* in rectangular PBRs showed that it was necessary to consider an intermediate zone in the PBR, with a particular relaxation metabolism, which could be

responsible in the high level of intracellular PHB accumulation (Cornet *et al.*, 1999; Cornet and Albiol, 2000). This hypothesis has led to establish two different global stoichiometries from a metabolic engineering approach (Favier *et al.*, 1999, and 2000; TN 45.4 and 49.1); one available in the illuminated zone of the PBR (as for *Spirulina*), and one available in the dark efficient zone of the PBR (short residence time).

The aim of this Technical Note is to verify if there is a satisfactory agreement between experimental results obtained in rectangular PBRs in a wide range of incident light fluxes and a proposed kinetic and stoichiometric model, based on the previous metabolic analysis. Because of the considered experimental results, the study is limited to the global conversion of carbon substrate in total biomass yields validation. Five carbon sources, which are the most representative of the output of the liquefying compartment, were used (acetate, propionate, butyrate, isovalerate, isobutyrate) to determine the effects of different substrates on growth kinetics in conditions of carbon substrate limitation.

This work relies on the experimental tests performed at UAB and reported in TNs 37.81-82 (Lenguaza *et al.*, 1998a and b).

1- Kinetic Model

The kinetic model used in this study was previously described in the TN 45.1 (Cornet *et al.*, 1999). It mainly relies on a knowledge model for radiative transfer description, i.e. a generalized monodimensional two-flux model, coupled with a zone model for volumetric kinetics averaging. The specific growth rate is given by postulating a Monod law relative to mean local light intensity:

$$\mathbf{m} = \mathbf{m}_M \frac{I_\Sigma}{K_J + I_\Sigma} \quad (1)$$

in which the constant K_J depends on pigment and antenna composition for each micro-organism, but is independent of the carbon substrate, whereas the maximum specific growth rate \mathbf{m}_M is obviously dependent on the carbon source (Cornet *et al.*, 1999).

Thus the mean volumetric growth rate in the reactor is given by:

$$\langle r_x \rangle = \frac{1}{V} \iiint_V r_x dV = \frac{1}{V} \iiint_V \mathbf{m}_M C_X \frac{I_\Sigma}{K_J + I_\Sigma} dV \quad (2)$$

In order to have constant kinetic parameters over a wide range of incident fluxes, and to provide fully predictive models, the integration must be performed on zones where metabolic activity occurs (Cornet *et al.*, 1992; Cornet *et al.*, 1995; Cornet *et al.*, 1999).

For photo-heterotrophic micro-organisms, the possibility exists of accumulating reducing power in the dark using the transmembrane potential to generate a reverse electron transfer (RET) from succinate to a final acceptor (NADH₂). From this RET, no additional light energy is necessary for the synthesis of storage intermediates such as polyhydroxybutyrate (PHB) or glycogen. However, in this case, ATP synthesis is not possible and such a mechanism can operate only for short dark residence times of cells. For higher dark residence times of cells, all metabolic activity is stopped if no proper electron acceptor is available, or if the residence time of cells remains too short to avoid appearance of a fermentative metabolism.

Consequently, it is necessary to divide the total volume of the reactor into three different metabolic zones to calculate the integral (2):

$$\langle r_x \rangle = (1 - \mathbf{b} - \mathbf{g}) \frac{1}{V_1} \iiint_{V_1} r_{x_1} dV + \mathbf{b} \frac{1}{V_2} \iiint_{V_2} r_{x_2} dV + \mathbf{g} \frac{1}{V_3} \iiint_{V_3} r_{x_3} dV \quad (3)$$

As illustrated in Figure 1, the volume V_3 is an illuminated zone in which the growth rate profile is given by coupling the radiative transfer equation with equation (1); The volume V_2 is a dark zone in which the residence time of the cells remains sufficiently short for metabolic activity to continue; and the volume V_1 is a dark zone where no significant biomass growth takes place, i.e. $r_{x_1} = 0$. For reactors illuminated on one side, the monodimensional approximation holds true and the volumetric integrals can be replaced by simple integrals in the z-direction and so the volumetric fractions \mathbf{b} and \mathbf{g} are given by (Figure 1):

$$\mathbf{g} = V_3/V = L_3/L \text{ and } \mathbf{b} = V_2/V = (L_2 - L_3)/L \quad (4)$$

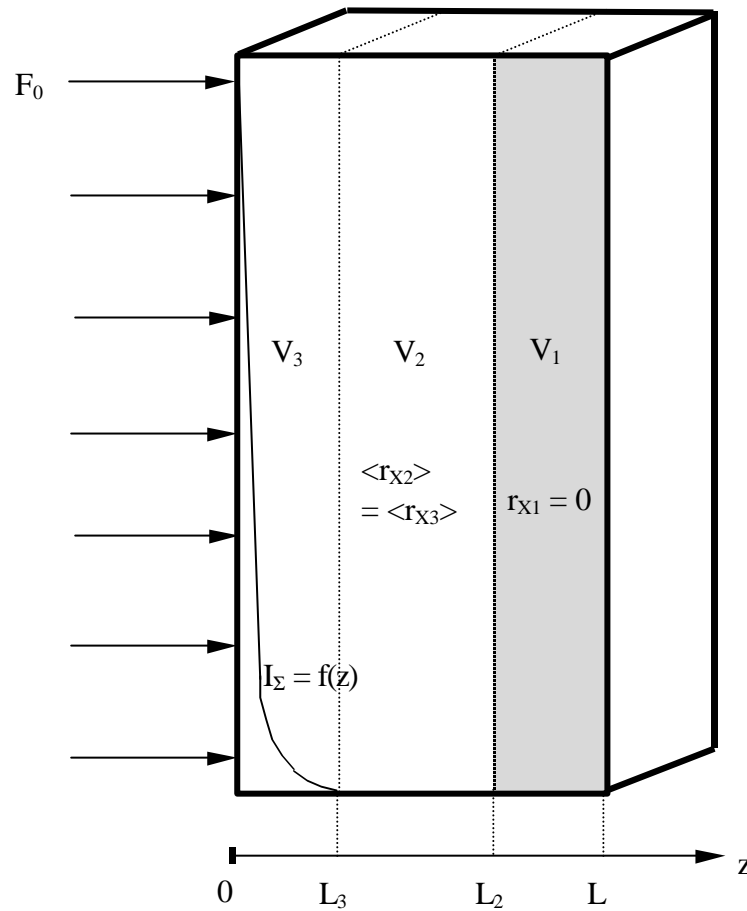


Figure 1: Definition of the three zones with different metabolic activity in modeling photoheterotrophic growth kinetics in rectangular photobioreactors illuminated from one side (incident flux F_0). The working illuminated volume is defined by the length L_3 and the volume V_3 . The intermediate zone with storage of reducing power in the dark is defined by the volume V_2 and the length $(L_2 - L_3)$. In the residual zone $(L - L_2)$, at the rear of the reactor, the volumetric biomass growth rate is zero.

The length L_3 , called the working illuminated volume, can be calculated in the same way as for *Spirulina*, from the knowledge of the mean efficient intensity E_J corresponding to the minimal radiant light energy at which photosynthesis remains efficient. The length L_2 can also be easily established because it splits the reactor volume into a metabolically active zone and an inefficient one. Consequently, it must be defined from the appearance of linear mean growth rate in batch

experiments. Finally, we assume that the mean volumetric growth rate in the dark zone is controlled by the volumetric growth rate in the working illuminated volume, i.e. that the intermediate zone corresponds to a relaxation mechanism i.e. a decay of the transmembrane potential insuring the RET. Equation (3) with equation (4) is then rewritten, for monodimensional approximation:

$$\langle r_x \rangle = fs_l (\mathbf{b} + \mathbf{g}) \frac{1}{L_3} \int_0^{L_3} r_{x_3} dV \frac{C_c}{K_c + C_c} = fs_l q \frac{1}{L} \int_0^{L_3} r_{x_3} dV \frac{C_c}{K_c + C_c} \quad (5)$$

where the illuminated surface fraction fs_l has been introduced to describe cases in which only part of the photoreactor surface is illuminated, and the Monod term with respect to carbon substrate concentration C_c enables to take into account kinetic effects of carbon source limitations. From this equation, the mean volumetric rate for carbon substrate consumption is easily calculated from the mass conversion yield $Y_{S/X}$:

$$\langle r_s \rangle = -Y_{S/X} \langle r_x \rangle \quad (6)$$

Equations (5-6) with equation (1) will be used for simulations given in the Results and Discussion section below. The model coefficients determined in TN 45.1 (Cornet *et al.*, 1999) under light limitation only and for the five main carbon substrates are given in Table 1.

Table 1: Summary of numerical values for light transfer and kinetic model coefficients.

Mean mass absorption coefficient	Ea	$270 \text{ m}^2.\text{kg}^{-1}$
Mean mass scattering coefficient	Es	$370 \text{ m}^2.\text{kg}^{-1}$
Mean efficient intensity for photosynthesis	E_j	$10^{-2} \text{ W}.\text{m}^{-2}$
Monod saturation constant for mean local intensity	K_j	$15 \text{ W}.\text{m}^{-2}$
Proportionality constant defining the efficient zone of the PBR	q	3
Maximum specific growth rate for carbon substrate	μ_{\max}	
Acetate	0.15 h ⁻¹	
Propionate	0.13 h ⁻¹	
Butyrate	0.115 h ⁻¹	

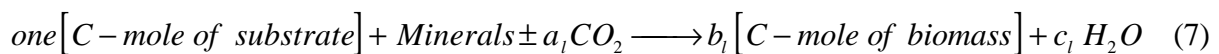
Isovalerate	0.07 h ⁻¹
Isobutyrate	0.07 h ⁻¹

2- Stoichiometries - Yields Calculations

The classical problem of substrate to biomass yield calculation $Y_{S/X}$ from stoichiometric equations when different metabolic zones exist is not so trivial. Two stoichiometries are here necessarily established: one for the working illuminated volume corresponding to the major cellular components synthesis, and one in the dark efficient zone, responsible in the PHB accumulation in cells. This work was performed respectively in TN 45.4 (Favier *et al.*, 1999) and TN 49.1 (Favier *et al.*, 2000).

2.1- Stoichiometries and Yields in the Illuminated Zone

From metabolic engineering and analysis, stoichiometric equations were previously established by Favier *et al.* (1999, TN 45.4) in the working illuminated zone for active biomass synthesis in the general form:

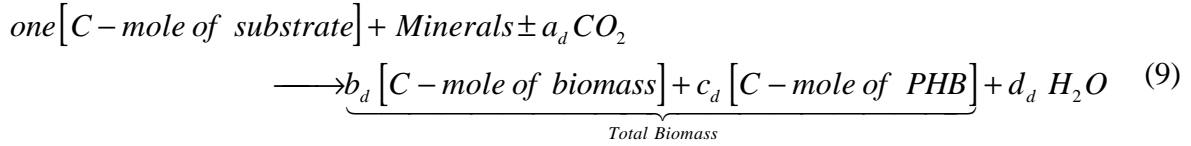


the mass substrate on active biomass yield in the illuminated zone $Y_{S/X(l)}$ is then defined from:

$$Y_{S/X(l)} = \frac{\text{mass of one C - mole of substrate}}{b_1 \times (\text{mass of one C - mole of biomass})} \quad (gS / gXA) \quad (8)$$

2.2- Stoichiometries and Yields in the Dark Efficient Zone

The dark efficient zone is supposed to correspond to PHB synthesis and accumulation. In the same way, stoichiometric equations were established (Favier *et al.*, 2000, TN 49.1) in the general form:



leading to the mass substrate on total biomass yield $Y_{S/X(d)}$ in the dark efficient zone definition:

$$Y_{S/X(d)} = \frac{\text{mass of one C - mole of substrate}}{b_d \times (\text{mass of one C - mole of biomass}) + c_d (\text{mass of one C - mole of PHB})} \quad (\text{gS / gXT}) \quad (10)$$

2.3- Mean Stoichiometries and Yields

Clearly, each of the previous stoichiometries must be averaged by weighting from the illuminated and dark zone fractions at any time in the photobioreactor. Because the fractions **g** and **b** are defined in regard to the total volume of the reactor (*V*), it is necessary to define fractions relative to the efficient volume of the PBR in which growth occurs (*V*₃ + *V*₂). These definitions are straightforward for the illuminated fraction *f*_{*V*(*l*)} (taking **g** ≤ 1 and (**b** + **g**) ≤ 1 and with *f*_{*V*(*l*)} + *f*_{*V*(*d*)} = 1):

$$f_{V(l)} = \frac{\mathbf{g}}{\mathbf{b} + \mathbf{g}} \quad (11)$$

and for the dark efficient fraction *f*_{*V*(*d*)}:

$$f_{V(d)} = \frac{\mathbf{b}}{\mathbf{b} + \mathbf{g}} \quad (12)$$

The mean global yield for total biomass synthesis (illuminated + dark zones) is then given by:

$$\boxed{Y_{S/X} = f_{V(l)} Y_{S/X(l)} + f_{V(d)} Y_{S/X(d)}} \quad (13)$$

It must be point out first that this global yield depends on light and dark volume fractions, i.e. it is time dependent in batch mode cultivation, and second that the proposed approach enables to predict the PHB percentage obtained in the total biomass at each time in batch mode or at steady state in continuous mode cultivation. The resulting global stoichiometries for total biomass (i.e. active biomass and PHB) are in fact easily calculated from the knowledge of the fractions $f_{V(t)}$ and $f_{V(d)}$ which relate the PHB cellular content to the culture conditions.

3- Materials and Methods

Experimental batch cultures were performed in rectangular photobioreactors (Roux flasks) of 1.1 L working volume. Cultures were grown in a set-up, enclosed in a dark chamber with black surfaces, arranged as depicted in Figure 2.

Illumination was arranged in monodimensional conditions. The lamps used were Sylvania professional 25 BAB 38°, 12V 20W. Different incident light fluxes were obtained by varying the length between the lamps and the reactor.

Mean incident fluxes of photosynthetically active radiation (PAR) were measured using a quantum sensor, (Licor Li-190SA), attached to an LI-189 portable meter. The sensor gives the photosynthetic photon flux density (PPFD) in $\mu\text{mol}\cdot\text{s}^{-1}\cdot\text{m}^{-2}$. Conversion of quantum units to radiometric units in the range 350-950 nm was carried out using a constant factor of 0.425 obtained from the emission spectrum of the lamps. These measurements were confirmed, using Reinecke salt as actinometer, to calculate the mean incident irradiation on the illuminated surface (Cornet *et al.*, 1997). Practically, for $f_{S_I} = 1$, i.e., the whole of the surface illuminated, we used a high value for the incident flux of $420 \text{ W}\cdot\text{m}^{-2}$, then a low value of $45 \text{ W}\cdot\text{m}^{-2}$.

Biomass dry weight was calculated from the measured absorbency of a sample (A_{700}) and its value interpolated on a calibration curve taken from previous determinations (Albiol 1994).

The bacterial strain *Rhodospirillum rubrum* (ATCC 25903) was obtained from the American Type Culture Collection. It was revived and subcultured for maintenance using the supplier's recommended media.

Experimental culture media were based on the basal salts mixture of Segers & Verstraete as described by Suhaimi (Suhaimi *et al.* 1987), using different carbon sources and biotin as the only vitamin. To maintain the pH of the culture media and to decrease medium culture precipitation, which could affect the measurements, the following modifications were made. Phosphate concentration was decreased to the following levels: KH_2PO_4 0.2 g/l K_2HPO_4 0.3 g/l. Buffer capacity to maintain the culture pH was obtained using 3-morpholino propane sulphuric acid (MOPS) 21 g/l. Phosphate was autoclaved separately. The pH was adjusted to 6.9. At the end of the culture the pH was found to be 7.4.

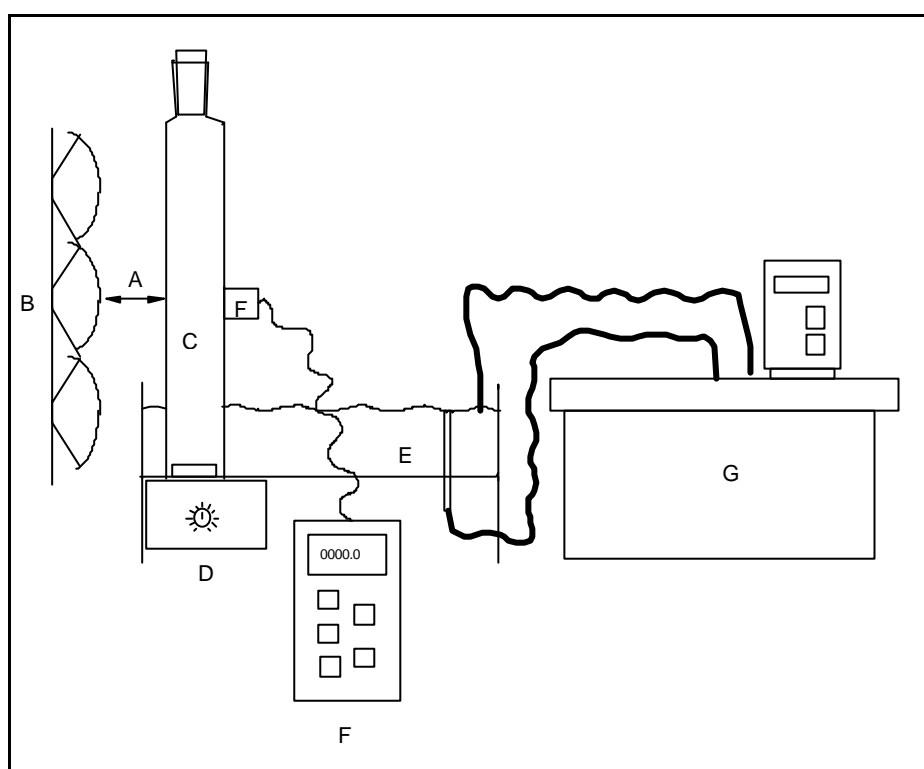


Figure 2: Experimental set-up; A: lamp-bioreactor distance. B: Lamp support. C: Bioreactor. D: magnetic stirrer. E: water bath. F: light sensor. G: thermostatic bath

The carbon sources used in these experiments were acetic acid (2.5 g/l), butyric acid (1.84 g/l), propionic acid (2.06 g/l), isovaleric acid (1.7 g/l) and isobutyric acid (1.84 g/l). The

concentrations used correspond to 1 gC/l for all cases. Sodium carbonate concentrations for each case were respectively 0.25 g/l, 1.35 g/l, 0.67 g/l, 1.23 g/l, 1.35 g/l in order to keep constant the ratio C/N = 5. In each experiment, carbon source was analyzed by a GPC method (HP 5890) until it was totally exhausted.

Temperature (30°C) was maintained using a water bath with heating and cooling capacities. The culture was kept homogeneous with a magnetic stirrer.

4- Results and Discussion

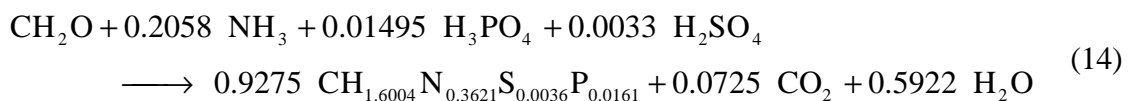
The results of simulations in rectangular PBRs discussed in this section are based on experimental results of Lenguaza *et al.* (1998a and b; TN 37.81 and 37.82). If there is no doubt that results at high fluxes (430 W.m⁻²) of TN 37.81 are available for modeling, it is not the case for results of TN 37.82 at low fluxes (45 W.m⁻²). In this technical note, clearly appears a problem of carbon recovery percentage since, depending of the experiments, values between 150 and 220 % have been calculated, leading to erroneous experimental values for the mass conversion yields. This problem was already pointed out by Favier *et al.* (2000), and by Cornet and Albiol (2000) in their publication on kinetic modeling of *Rs. rubrum*. It is now well established that intracellular granules of PHB accumulated strongly modify the mean refractive index of cells (this effect was verified in the lab using Lorentz-Mie theory calculations) and then the scattering coefficient which is responsible of light attenuation in optical density measurements at non-absorbed wavelength. Besides, this fact was used by some authors to established relations between optical density and PHB content in cells (Wilde, 1962; Lopatin *et al.*, 1996)! Clearly, PHB accumulation in cells at low fluxes explains the erroneous relation used in TN 37.82 between OD₇₀₀ and dry mass. ***Consequently, we have proposed in this study to recalculate dry weight data (total biomass) obtained in TN 37.82 from the basis that the carbon recovery percentage was 100% when the carbon substrate was totally exhausted.*** We have made exactly the same correction in the recent paper of Cornet and Albiol (2000) for kinetic modeling of *Rs. rubrum* under light limitation only, and also in Table 4 of TN 49.1 (Favier *et al.*, 2000).

One of the aim of this work was also to determine the Monod saturation constant K_C (equation 5) for each of the five main carbon substrates considered. Clearly, as it was already demonstrated on *Spirulina platensis* studies (e.g. for nitrate limitation), it is only a preliminary assessment of this constant on batch experiments; the exact value needing to be determined in continuous culture mode. ***It appeared from this preliminary analysis that the same value of K_C seems to correspond for all the carbon substrates considered in this paper. Consequently, all the simulations hereafter presented use the value $K_C = 10^{-1}$ g/l for the considered carbon substrate.***

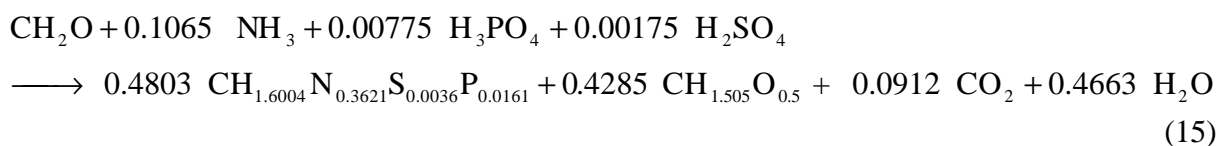
Finally, as it was already explained in TN 45.1 (Cornet *et al.*, 1999), most of the experiments performed in TN 37.81-37.82 presents lag phases, corresponding to more or less understood phenomena (pigment content modifications?). The proposed model of course is unable to take into account such non-reproducible features and the experimental data considered for this study correspond only to growth phases. Moreover, for few experiments, the initial value of carbon substrate concentration measured was not in agreement with the other data time course; in this case, this value was identified in order to obtain a best resulting simulation.

4.1- Acetate as Carbon Substrate

For acetate as main carbon source, the following stoichiometric equations were obtained in the light zone (Favier *et al.*, 1999):



and in the dark operative zone (Favier *et al.*, 2000):



leading to the following values of yields:

$$\begin{aligned} Y_{S/X(l)} &= 1.408 \\ Y_{S/X(d)} &= 1.477 \end{aligned} \quad (16)$$

Numerical simulations obtained with these theoretical yields, together with equations (5,6 and 13), and with $K_C = 10^{-1}$ g Acetate/l are given with experimental data on Figures 3a and b for high and low incident light fluxes.

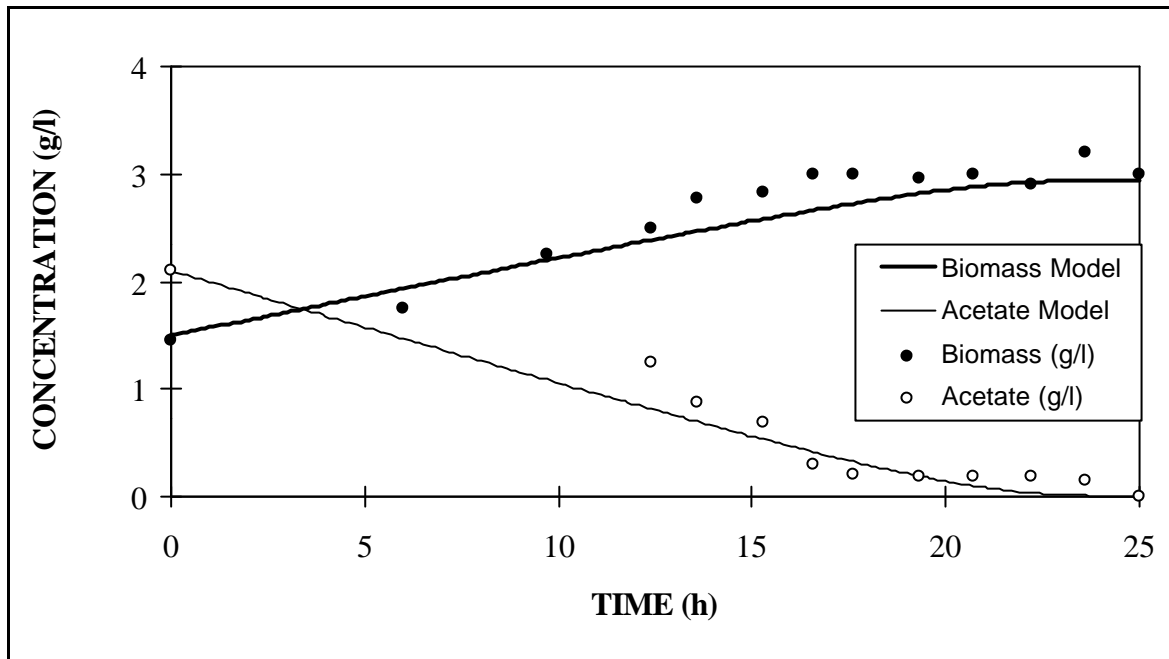


Figure 3a: Time course for total biomass and acetate concentrations in rectangular PBR illuminated on one side with an incident flux $F_0 = 420 \text{ W.m}^{-2}$. Comparison with the proposed stoichiometric and kinetic model.

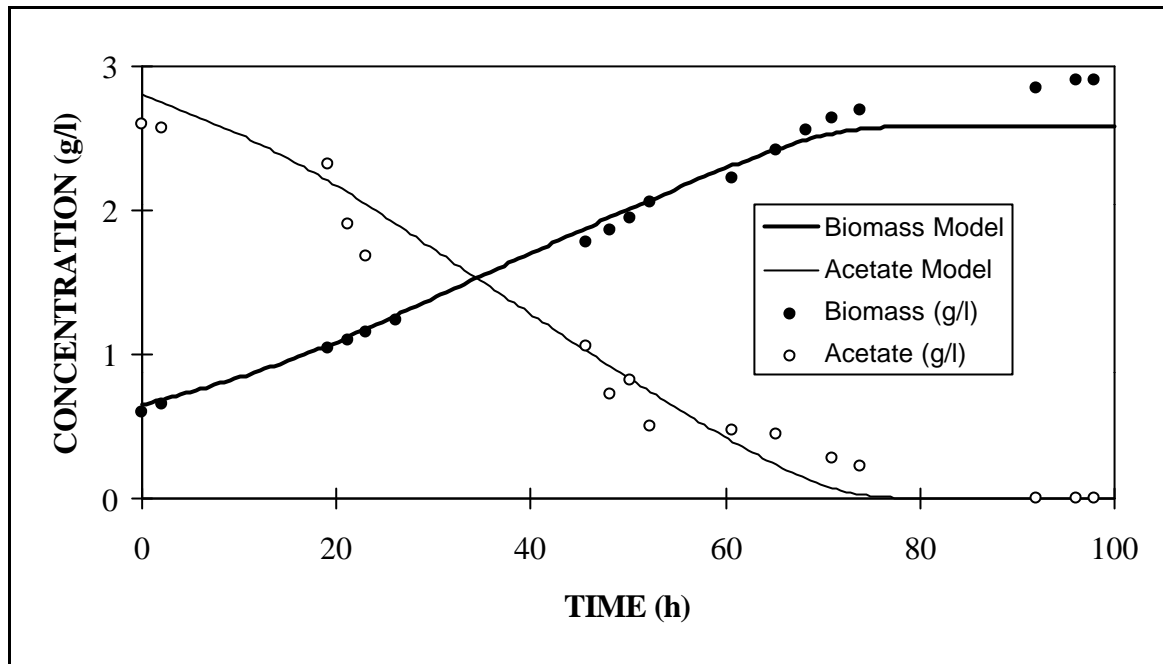
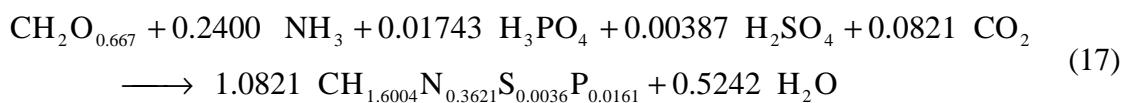


Figure 3b: Time course for total biomass and acetate concentrations in rectangular PBR illuminated on one side with an incident flux $F_0 = 45 \text{ W.m}^{-2}$. Comparison with the proposed stoichiometric and kinetic model.

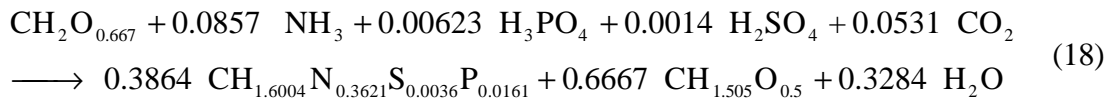
Clearly, the Figures show a good agreement between model and experiment, validating the mass acetate conversion yields given by eq. (13, 16), in a range of incident light fluxes varying by a factor 10.

4.2- Propionate as Carbon Substrate

For propionate as main carbon source, the following stoichiometric equations were obtained in the light zone (Favier et al., 1999):



and in the dark operative zone (Favier et al., 2000):



leading to the following values of yields:

$$Y_{S/X(l)} = 0.971 \quad (19)$$

$$Y_{S/X(d)} = 1.061$$

Numerical simulations obtained with these theoretical yields, together with equations (5,6 and 13), and with $K_C = 10^{-1}$ g Propionate/l are given with experimental data on Figures 4a and b for high and low incident light fluxes.

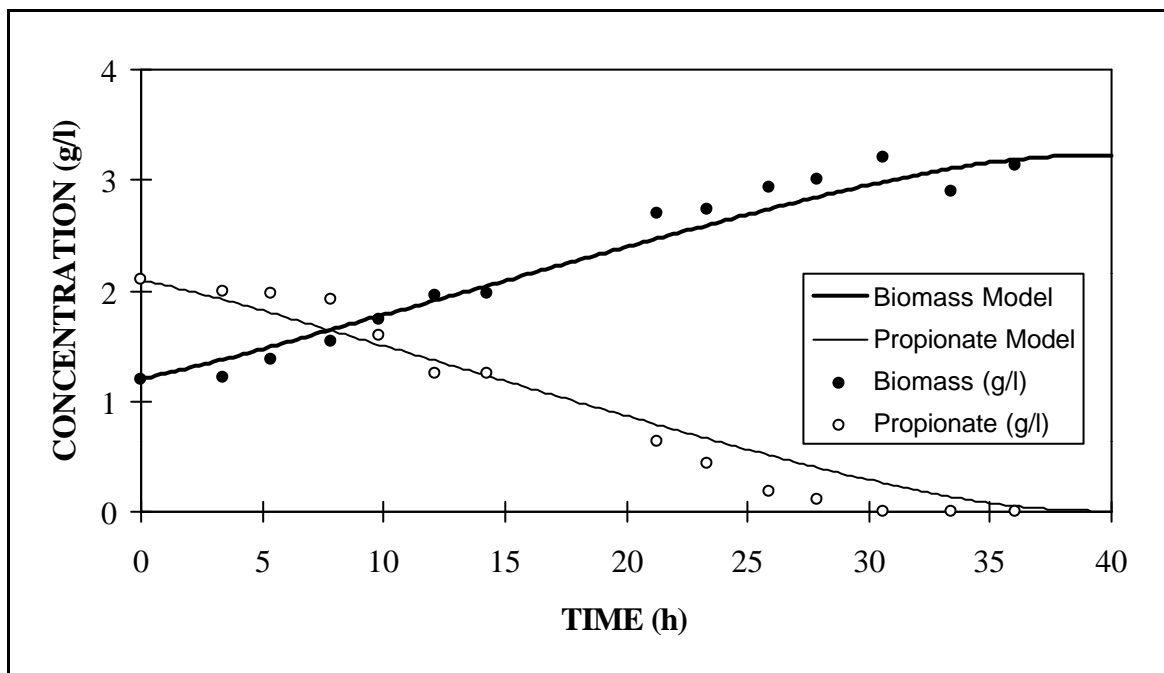


Figure 4a: Time course for total biomass and propionate concentrations in rectangular PBR illuminated on one side with an incident flux $F_0 = 420 \text{ W.m}^{-2}$. Comparison with the proposed stoichiometric and kinetic model.

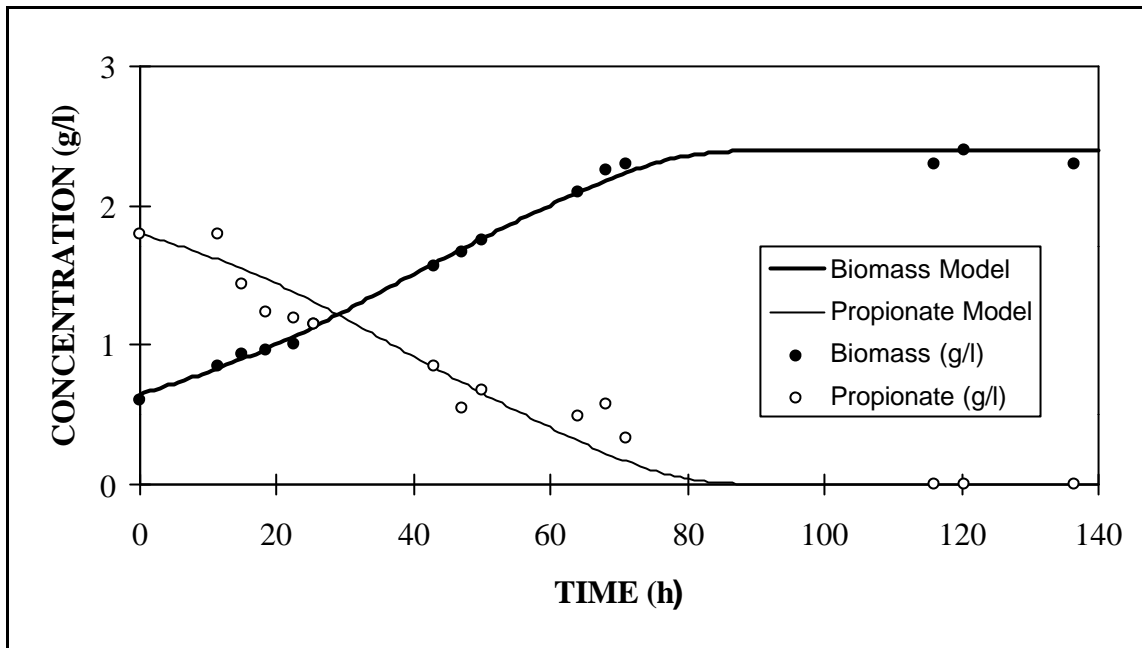
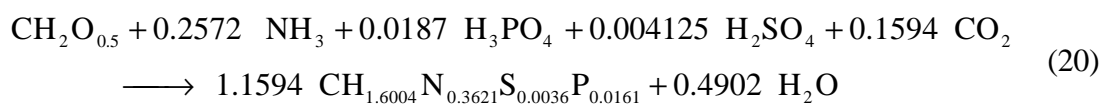


Figure 4b: Time course for total biomass and propionate concentrations in rectangular PBR illuminated on one side with an incident flux $F_0 = 45 \text{ W.m}^{-2}$. Comparison with the proposed stoichiometric and kinetic model.

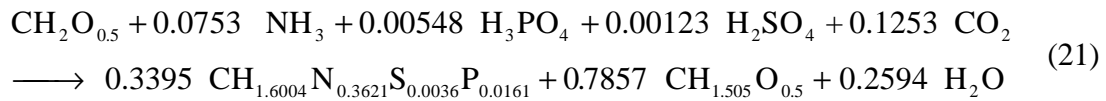
Clearly, the Figures show a good agreement between model and experiment, validating the mass propionate conversion yields given by eq. (13, 19), in a range of incident light fluxes varying by a factor 10.

4.3- Butyrate as Carbon Substrate

For Butyrate as main carbon source, the following stoichiometric equations were obtained in the light zone (Favier et al., 1999):



and in the dark operative zone (Favier et al., 2000):



leading to the following values of yields:

$$Y_{S/X(l)} = 0.820$$

$$Y_{S/X(d)} = 0.889 \quad (22)$$

Numerical simulations obtained with these theoretical yields, together with equations (5,6 and 13), and with $K_C = 10^{-1}$ g Butyrate/l are given with experimental data on Figures 5a and b for high and low incident light fluxes.

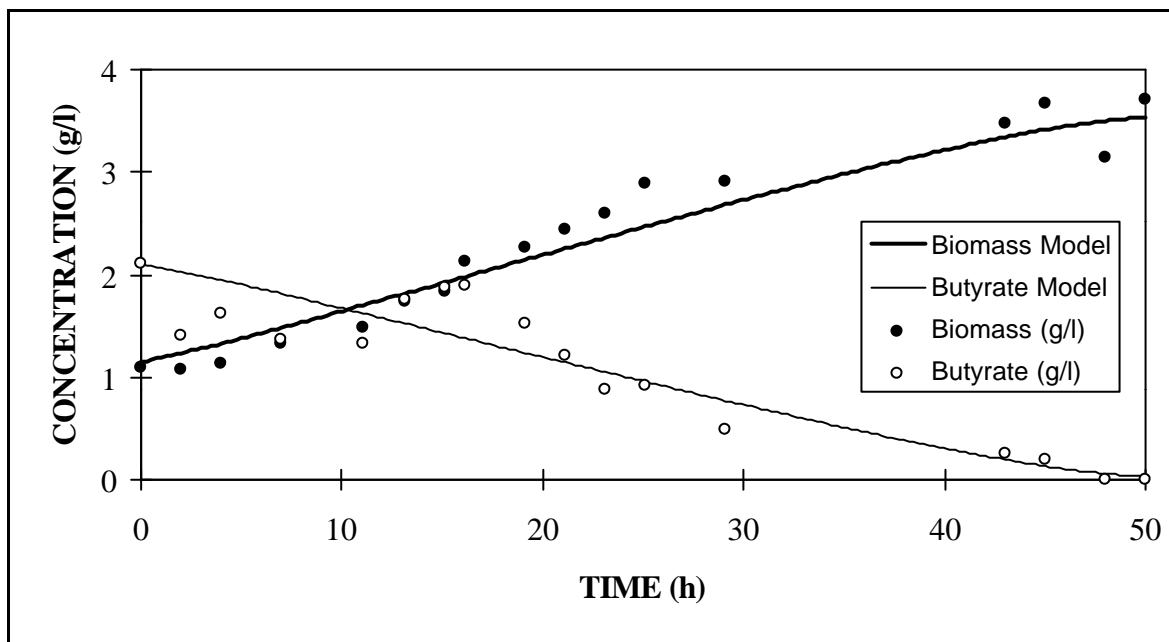


Figure 5a: Time course for total biomass and butyrate concentrations in rectangular PBR illuminated on one side with an incident flux $F_0 = 420 \text{ W}\cdot\text{m}^{-2}$. Comparison with the proposed stoichiometric and kinetic model.

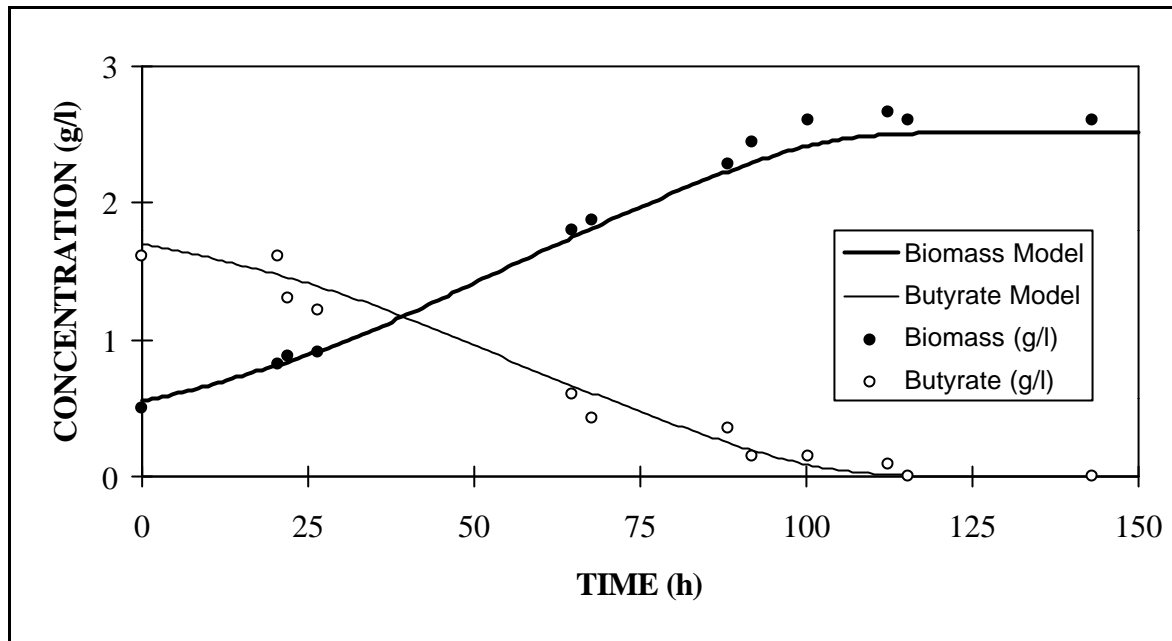
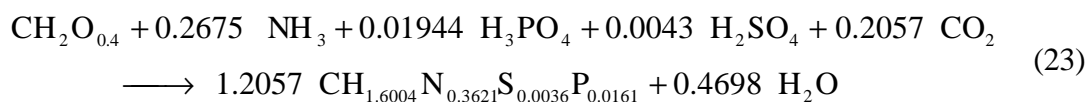


Figure 5b: Time course for total biomass and butyrate concentrations in rectangular PBR illuminated on one side with an incident flux $F_0 = 45 \text{ W.m}^{-2}$. Comparison with the proposed stoichiometric and kinetic model.

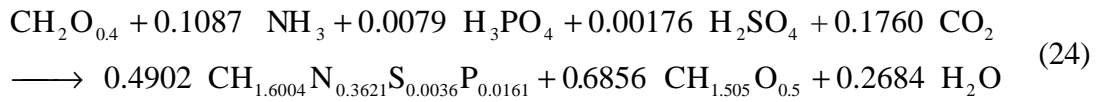
Clearly, the Figures show a good agreement between model and experiment, validating the mass butyrate conversion yields given by eq. (13, 22), in a range of incident light fluxes varying by a factor 10.

4.4- Isovalerate as Carbon Substrate

For Isovalerate as main carbon source, the following stoichiometric equations were obtained in the light zone (Favier et al., 1999):



and in the dark operative zone (Favier et al., 2000):



leading to the following values of yields:

$$\begin{aligned} Y_{S/X(l)} &= 0.735 \\ Y_{S/X(d)} &= 0.783 \end{aligned} \quad (25)$$

Numerical simulations obtained with these theoretical yields, together with equations (5,6 and 13), and with $K_C = 10^{-1}$ g Isovalerate/l are given with experimental data on Figures 6a and b for high and low incident light fluxes.

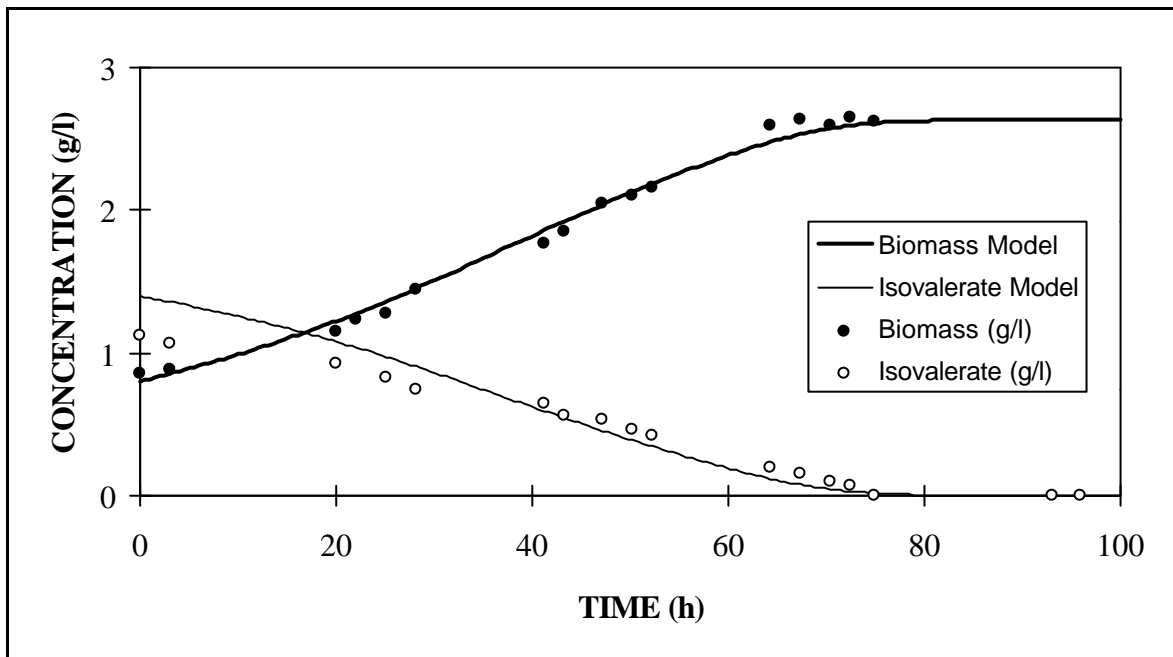


Figure 6a: Time course for total biomass and isovalerate concentrations in rectangular PBR illuminated on one side with an incident flux $F_0 = 420 \text{ W.m}^{-2}$. Comparison with the proposed stoichiometric and kinetic model.

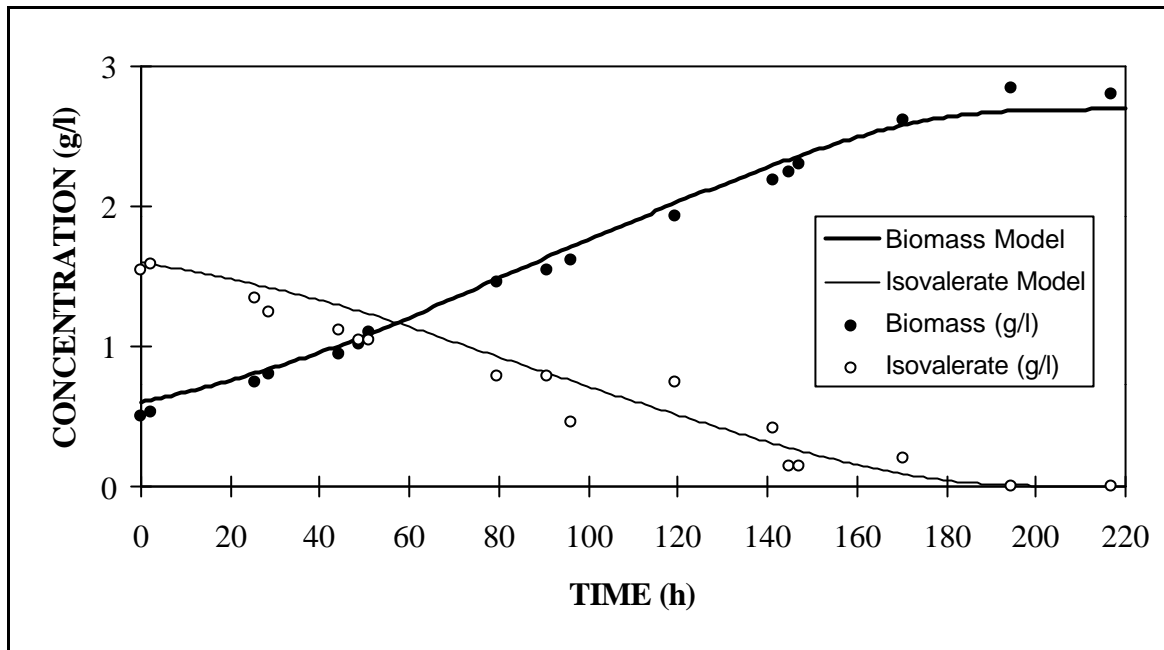


Figure 6b: Time course for total biomass and isovalerate concentrations in rectangular PBR illuminated on one side with an incident flux $F_0 = 45 \text{ W.m}^{-2}$. Comparison with the proposed stoichiometric and kinetic model.

Clearly, the Figures show a good agreement between model and experiment, validating the mass isovalerate conversion yields given by eq. (13, 25), in a range of incident light fluxes varying by a factor 10.

4.5- Isobutyrate as Carbon Substrate

As previously explained (Favier *et al.*, 1999 and 2000), isobutyrate presents the same global stoichiometric formula as butyrate. The two stoichiometric equations in light and dark zones, and the two mass conversion yields are then given by equations (20-22); only the maximum specific growth rate is strongly affected (Table1). Moreover, because this substrate seems to lead to a photoinhibition phenomenon at high fluxes (Lenguaza *et al.*, 1998a), experimental results were obtained only at low flux (Lenguaza *et al.*, 1998b).

Numerical simulation at light flux of 45 W.m^{-2} and with the same previous value for K_C is given on Figure 7.

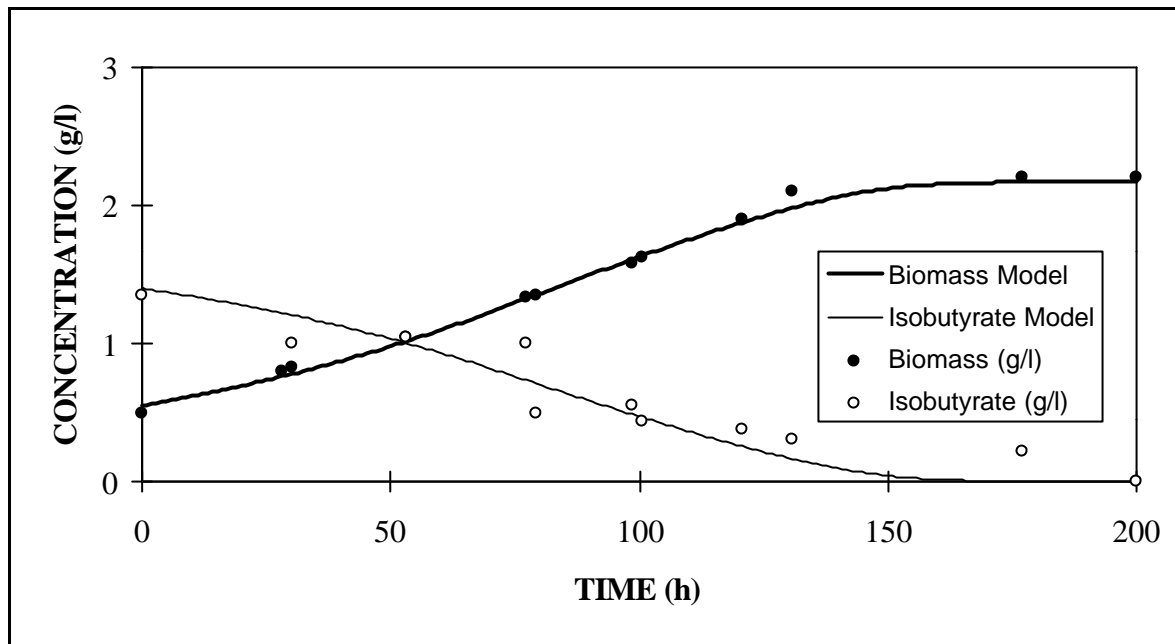


Figure 7: Time course for total biomass and isobutyrate concentrations in rectangular PBR illuminated on one side with an incident flux $F_0 = 45 \text{ W.m}^{-2}$. Comparison with the proposed stoichiometric and kinetic model.

The Figure still shows a good agreement between model and experiment, validating the mass isobutyrate conversion yields given by eq. (13, 22).

Generally, one observes a close agreement between experimental data and stoichiometric and kinetic model for each carbon substrate investigated. This is not so surprising for two main reasons:

- The kinetic model was previously validated under light limitation only on the same experiments but on the first growth phase, before carbon limitation appearance (Cornet *et al.*, 1999; Cornet and Albiol, 2000);
- The stoichiometric analysis from metabolic engineering (Favier *et al.*, 1999 and 2000) approach proved that the mass conversion yields for carbon substrate were very insensitive to the

culture conditions and PHB accumulation (many different metabolic hypotheses lead to the same yields). It is easily verified in this study that the values of $Y_{S/X(l)}$ and $Y_{S/X(d)}$ are quite close.

As a consequence of this last remark, it must be emphasized that the good agreement obtained here from carbon substrate to total biomass conversion does not be considered as a validation of the zone model and of the stoichiometric equations established for the short residence time of cells at obscurity (Favier *et al.*, 2000). It will be clearly feasible only by complete analysis of the biomass quality produced in continuous culture conditions (and especially from the accurate knowledge of the PHB content), coupled with the knowledge of kinetic rates and volume fractions (illuminated, dark efficient and dark inoperative) in the PBR.

Continuous cultures under light and carbon limitations will be also necessary to investigate with accuracy the Monod constant for carbon substrates. The constant value of 10^{-1} g/l proposed in this TN, determined in batch functioning, clearly corresponds to a maximum value, but the actual value could be considerably lower (as an example, the nitrate Monod constant for *S. platensis* determined from many accurate batch experiments has been proved ten times higher than the actual one determined later at UAB in continuous cultures).

Conclusions and Perspectives

A kinetic and stoichiometric zone model for photoheterotrophic growth of micro-organisms has been proposed in this Technical Note, with a transient and specific metabolism in a dark efficient zone. Indisputably, it is a new and original approach. It has been validated first under light limitation only from total biomass growth rate measurements, and second from coupling with rates for the five main carbon substrates of *Rs. rubrum* in batch cultures and in rectangular PBRs. Very good agreement has been obtained between model and experiments but the strong weakness of this study relies on the lack of knowledge in the quality composition of the produced total biomass. Clearly, investigate short transient metabolism in such micro-organisms is a quite fundamental task, far from the engineering approach of the MELiSSA team. The sole possibility to macroscopically validate this hypothesis is to measure with accuracy the rates of PHB accumulation corresponding to situations in which the different zones (i.e. the incident light flux and the biomass concentration) are known and controlled. It is then only feasible in continuous culture conditions, and such a considerable work remains to be performed, first in validating the approach under light limitation only, and second in adding effects of carbon limitations.

Notations

C_C	Carbon substrate concentration (kg.m^{-3} or g.l^{-1})
C_X	Total biomass concentration (kg.m^{-3} or g.l^{-1})
E_a	Mean Schuster mass absorption coefficient ($\text{m}^2.\text{kg}^{-1}$)
E_J	Mean efficient intensity (W.m^{-2})
E_s	Mean Schuster mass scattering coefficient ($\text{m}^2.\text{kg}^{-1}$)
f_{sI}	Illuminated surface fraction for the PBR (dimensionless)
f_v	Volume fraction for the PBR (dimensionless)
F_0	Mean incident light flux (W.m^{-2})
I_Σ	Mean local available radiant light energy (W.m^{-2})
K_C	Half saturation constant relative to the carbon substrate (kg.m^{-3} or g.l^{-1})
K_I	Half saturation constant relative to the mean incident light (W.m^{-2})
L	Length of the photoreactor (m)
$q=L_2/L_3$	Proportionality constant between illuminated and dark operative volumes (dimensionless)
r_s	Local volumetric carbon source consumption rate ($\text{kg.m}^{-3}.\text{h}^{-1}$)
r_x	Local volumetric biomass growth rate ($\text{kg.m}^{-3}.\text{h}^{-1}$)
t	Time (h)
V	Volume (m^3)
$Y_{S/X}$	Mass carbon substrate to biomass conversion yield (dimensionless)
$\langle \rangle = \frac{1}{V} \iiint_V dV$	Mean volumetric integral quantity (dimensionless)

Greek letters

β	Dark operative volume fraction (dimensionless)
γ	Working illuminated volume fraction (dimensionless)
μ	Specific growth rate (h^{-1})

μ_M Maximum specific growth rate (h^{-1})

Subscripts

- (l) Relative to the illuminated zone volume in the PBR
- (d) Relative to the dark efficient zone volume in the PBR
- 1 For dark zone with no metabolic activity in the PBR
- 2 For dark operative intermediate zone in the PBR
- 3 For working illuminated zone in the PBR

References

- Acien Fernandez F. G., Garcia Camacho F., Sanchez Perez J. A., Fernandez Sevilla J.M., Molina Grima E. 1997.** A model for light distribution and average solar irradiance inside outdoor tubular photobioreactors for the microalgal mass culture. *Biotech. Bioeng.*, 55: 701-714.
- Aiba S. 1982.** Growth kinetics of photosynthetic micro-organisms. *Adv. Biochem. Eng.*, 23: 85-156.
- Albiol J. 1994.** Study of the MELISSA photoheterotrophic compartment. Kinetics and effects of C limitation. In: *ESA report ESA-EWP-1808. ESA/YCL/2148.JAS.*
- Cassano A. E., Martin C. A., Brandi R.J., Alfano O. M. 1995.** Photoreactor analysis and design: Fundamentals and Applications. *Ind. Eng. Chem. Res.* 34: 2155-2201.
- Cornet J.-F., Dussap C.G., Dubertret G. 1992.** A structured model for simulation of cultures of the cyanobacterium *Spirulina platensis* in photobioreactors: I. Coupling between light transfer and growth kinetics. *Biotech. Bioeng.*, 40: 817-825.
- Cornet J.-F., Dussap C.G., Gros J.-B., Binois C., Lasseur C. 1995.** A simplified monodimensional approach for modelling coupling between radiant light transfer and growth kinetics in photobioreactors. *Chem. Eng. Science.* 50: 1489-1500.
- Cornet J.-F. 1998.** Analysis of a photobioreactor performances for sizing a consumer compartment. In: *Technical note 1.1, ESA contract 12443/97/NL/PA, MELiSSA demonstration breadboard, Biorat.*
- Cornet J.F., Dussap C.G., Gros J.B. 1998.** Kinetics and Energetics of Photosynthetic micro-organisms in Photobioreactors. *Adv. Biochem. Eng./Biotech.* 59: 153-224.
- Cornet J.-F., Dussap C.G., Leclercq J.-J. 1999.** Simulation and model based predictive control of photobioreactors. In: *Proceedings of the ninth European Congress in Biotechnology (ECB9), July 1999, Bruxelles.*
- Cornet J.-F., Dussap C.G., Gros J.-B. 1999.** Kinetic modeling of *Rhodospirillum rubrum* growth in rectangular photobioreactors. In: *Technical note 45.1, ESA contract 12923/NL/MV.*
- Cornet J.-F., Albiol J. 2000.** Modeling photoheterotrophic growth kinetics of *Rhodospirillum rubrum* in rectangular photobioreactors. *Biotech. Prog.* In press.
- Favier L., Pons A., Poughon L. 1999.** Stoichiometric analysis of *Rs. rubrum* growth on different carbon substrates. In: *Technical note 45.4, ESA contract 13323/98/NL/MV.*
- Favier L., Poughon L., Cornet J.-F., Dussap C.G. 2000.** Stoichiometric analysis of *Rs. rubrum* growth for transient and short residence time in a dark operative zone. In: *Technical note 49.1, ESA contract 12924/98/NL/MV.*
- Lenguaza B., Albiol J., Godia F. 1998a.** Scientific tests for *Rs. rubrum* growth on different C sources - Part I. In: *Technical note 37.81, ESA contract 11549/95/NL/FG.*
- Lenguaza B., Albiol J., Godia F. 1998b.** Scientific tests for *Rs. rubrum* growth on different C sources - Part II. In: *Technical note 37.82, ESA contract 11549/95/NL/FG.*
- Lopatin V.N., Volova T.G., Shapovalov K.A., Shchur L.A. 1996.** Optical characteristics of cells of hydrogen-reducing bacteria accumulating polyhydroxybutyrate. *J. App. Spectr.* 63: 330-332.
- Suhaimi M., Liessens J., Verstraete W. 1987.** NH_4^+ -N Assimilation by *Rhodobacter capsulatus* ATCC 23782 grown axenically and non axenically in N and C rich media. *J. App. Bacteriol.* 62: 53-64.
- Wilde E. 1962.** Untersuchungen über wachstum und speicherstoffsynthese von *Hydrogenomonas*. *Arch. Mikrobiol.* 43: 109-137.